# Interfacial Alkane Films

T. K. Xia, Jian Ouyang, M. W. Ribarsky, and Uzi Landman
*School of Physics, Georgia Institute of Technology, Atlanta, Georgia 30332*
(Received 3 February 1992)

Adsorbed *n*-hexadecane films of thicknesses ~10, 20, and 40 Å are studied at 350 K via molecular-dynamics simulations. In the thickest film periodic oscillations of the density extend to ~18 Å from the solid-liquid interface, the roughness fluctuations at the liquid-vapor interface are Gaussian, and the density tail is fitted by an error function. Molecules in the first adsorbed layer lie preferentially parallel to the surface exhibiting domains of intermolecular orientational alignment. The diffusion is anisotropic with the component parallel to the surface greatly enhanced in the liquid-vapor region.

PACS numbers: 68.15.+e, 36.20.Ey, 61.20.Ja, 61.41.+e

The structural and dynamical properties of interphase interfaces (solid to liquid and liquid to vapor) of adsorbed molecular thin films are of both fundamental and applied interest in diverse areas (such as statistical mechanics of complex fluids, thin-film boundary lubrication, and coatings) and have been the subject of recent experimental and theoretical investigations [1–6]. While early theoretical studies of interfacial systems treated mostly adsorbed simple fluids [7] more recently increased attention has been focused on molecularly complex systems.

In this study we investigated, using molecular-dynamics simulations, evolutionary trends of the structure and certain aspects of the dynamics of *n*-hexadecane ($C_{16}H_{34}$) films of variable thickness adsorbed at 350 K on a crystalline substrate [modeling Au(001)]. In our simulations the alkane system was described via intramolecular and intermolecular interaction potentials developed previously [8], and the interaction between the pseudo-atoms ($CH_2$ and terminal $CH_3$ segments) and the substrate atoms was taken as a 6-12 Lennard-Jones potential with a length parameter $\sigma = 3.28$ Å, and a well depth parameter $\epsilon = 0.429$ kcal/mole (which is 3 times larger than that used in describing the hexadecane system itself) determined by fitting to experimentally estimated adsorption energies [9]. The calculational cell of area equal to $3.745 \times 10^3$ Å$^2$ (i.e., linear dimension of 61.2 Å) was periodically repeated in the $x$-$y$ directions and no periodicity was applied along the film thickness ($z$) direction. The static crystalline substrate was set in the geometry of a (001) gold surface consisting of three layers, with the lattice parameter of gold (the dynamics of the gold surface appears to have no discernable effect on the properties of the liquid film).

The equations of motion were integrated using Gear's fifth-order predictor-corrector with a time step $\Delta t = 2 \times 10^{-3}\tau$, where $\tau = 1.93$ ps (for the thickest film $\Delta t = 1 \times 10^{-3}\tau$). The simulations were performed in the canonical ensemble, with the temperature controlled via infrequent scaling of particles' velocities. Following a prolonged ($\sim 10^3$ ps) initial equilibration stage (which involved first turning off the attraction to the substrate and subsequently allowing molecules to adsorb on the surface by turning on the attraction), each equilibrium simulation lasted for another $10^3$ ps. Results were averaged over the last 250 ps of each run.

Segmental density profiles [$\rho_s(z)$] for three adsorbed film thicknesses, plotted versus distance from the center of atoms in the first layer of the solid surface, are displayed in Fig. 1(a). The solid-to-liquid (sl) interface is characterized by a regularly spaced oscillatory profile of the film segmental density, with the amplitude of the density oscillations decreasing away from the solid sur-

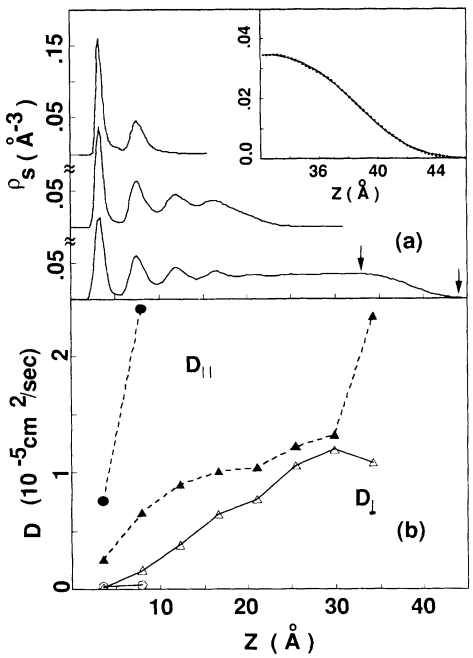


FIG. 1. (a) Segment density profiles for three thicknesses of adsorbed *n*-hexadecane films, plotted vs distance ($z$) from the solid surface, with the origin at the center of atoms in the top layer of the solid substrate. An error-function fit for the tail region (marked by arrows) of the thickest film is shown in the inset. (b) Diffusion constants in the directions parallel ($D_\parallel$) and perpendicular ($D_\perp$) to the surface plotted vs distance ($z$). Circles and triangles correspond to the thinnest (~10 Å) and thickest (~40 Å) films, respectively. Solid symbols denote $D_\parallel$ and empty ones correspond to $D_\perp$. Note enhancement of $D_\parallel$ in the tail region.

face, and extending up to 18 Å into the film. (Curiously, the range of density oscillations in the adsorbed film is similar to the range of measured oscillatory forces between mica surfaces across hexadecane [10].) Note that for the thickest film, past the fourth oscillation, the density achieves a value similar to that of bulk hexadecane. While the range and amplitude of density oscillations may depend somewhat on the nature of liquid-to-solid interactions (bonding strength and other characteristics, such as angular dependent versus central force interaction, etc.) liquid layering at sl interfaces appears to be a general phenomenon characteristic of the nature of atomic packing of liquids near a solid boundary. We note, however, that surface roughness and/or complex molecular structures (such as branched molecules) may obliterate the sl density oscillations [11]. An error-function [7(e)] fit,

$$\rho_s(z) = 0.5(\rho_l + \rho_v) - 0.5(\rho_l - \rho_v)\mathrm{erf}((z - z_0)/(2w_\rho)^{1/2}),$$

to the tail region of the thickest film (with $\rho_v = 0$) is shown in the inset with the fit parameters $w_\rho \simeq 2.95$ Å, $z_0 = 38.63$ Å, and $\rho_l = 0.86$ g/cm$^3$. Additionally we find that the surface tension (22.3 dyne/cm) calculated for films as thin as ~40 Å is in agreement with experiment [12] (22.58 ± 0.1 dyne/cm at 80 °C).

The liquid-to-vapor (lv) interface of the films appears "rough" (see Fig. 2, for the 10- and 20-Å-thick films, with similar results for the 40-Å film). The equilibrium average segmental distribution of the $z$-height fluctuations for the 20- and 40-Å-thick films can be fitted well by a Gaussian $(w\sqrt{2\pi})^{-1}\exp[-(z - z_0)^2/2w^2]$ with $w \simeq 2.96$ Å. It is interesting to note that the joint observation of a Gaussian height distribution and an error-function density profile of the lv interface may imply a short correlation length at the surface region of the molecular liquid film [7(e)]. In this context we remark that the shape of the lv interfacial density tail of long-chain molecules (polymers) is predicted to obey a $z^{-\mu}$ law with $\mu = \frac{4}{3}$ on the basis of a self-similarity argument [5], or $\mu = 2$ [6]. The question at what size a crossover to the long-chain regime occurs remains open.

Snapshots of typical molecular configurations for the thin and intermediate thickness films shown in Fig. 2(a) illustrate the "compact" structure of the first interfacial layer and molecular configurations bridging the second film layer and the (lv) interface in the 20-Å film. These properties are further quantified via plots of the conditional segmental distributions [13] shown in Fig. 2(b), where $f_l^e(z)$ expresses the normalized probabilities for one end of a molecule (terminal segment 1 or 16) to be located in layer $l$ of the film and the other end to be located in a region centered about $z$. As seen, while $f_1^e = \int_{l=1} f_1^e(z)dz \simeq 0.78$, i.e., $\approx 78\%$ of the molecules in the first layer have both ends located in that layer (a similar result was found for all three thicknesses), for molecules in the 20-Å-thick film with one end in the second layer, the probability, $f_2^e$, for finding the other end of the molecule in the lv tail region is 0.33 (i.e., 33% of the molecules bridge the second layer and the lv interface). In addition cross-layer molecular configurations

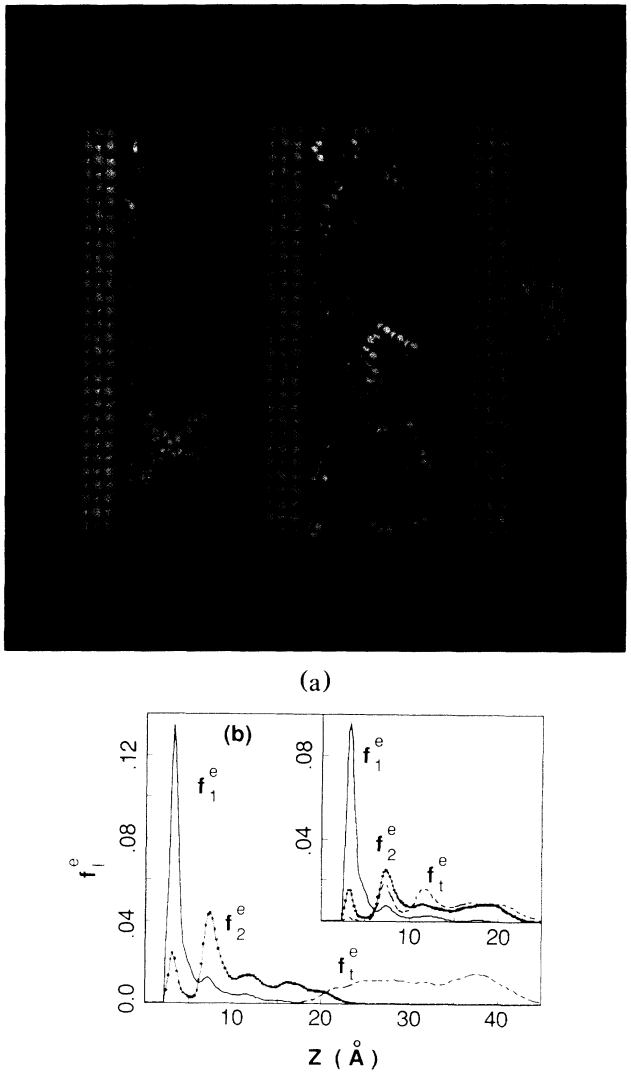


FIG. 2. (a) Molecular configurations of the thinnest (~10 Å, top) and intermediate thick (~20 Å, middle) adsorbed $n$-hexadecane films (side views). Molecules are differentiated by colors. Note the compactness of the first adsorbed layer at the sl interface, and the "rough" appearance of the lv interface. Shown at the bottom is a molecular configuration of the ~20-Å-thick adsorbed film depicting the first adsorbed layer, and only the bridging molecules with one end at the second layer and the other end located in the tail region (lv interface). (b) Conditional probabilities $f_l^e(z)$ for finding one end of a molecule in layer $l$, and the other end in a region about $z$, for the thick ($z \sim 40$ Å) adsorbed film. The dashed line corresponds to $f_t^e$, the probability for one end of the molecule to be located in the lv tail region and the other end about $z$ inside the film. Results for the intermediate thickness film (~20 Å) are shown in the inset.

are abundant (see in particular $f_1^e$ and $f_2^e$) and a significant fraction of the molecules in the lv tail region bridge that interface with the interior of the film (see $f_t^e$).

The in-plane structure in the first adsorbed layer is illustrated in Fig. 3(a) exhibiting straight (or nearly straight) chain configurations forming domains of intermolecular orientational order, as well as other L- and U-shaped molecular conformations. For all three film thicknesses the density in the first layer is $\sim 1.16$ g/cm$^3$, significantly higher than that in the bulklike region of $\sim 0.84$ g/cm$^3$ [see thick film in Fig. 1(a)]. The degrees of in-plane orientational order can be analyzed [3] via

$$g_{nm}^{l}(r) = g_{00}^{l}(r)\langle \cos(n\theta_1)\cos(m\theta_2) - \sin(n\theta_1)\sin(m\theta_2)\rangle_{\text{shell},l},$$

where $r$ is the magnitude of the vector $\mathbf{r}_{12}$ connecting the molecular center of mass of molecules 1 and 2 in layer $l$, projected onto the $x$-$y$ plane, and $\theta_i$ is the angle between the surface projection of the axial vector of molecule $i$, defined in terms of the inertia tensor or the end-to-end vector, and the projected $\mathbf{r}_{12}$. Results are averaged over molecules whose projected center of mass lies in a shell $(r, r+\Delta r)$. $g_{00}^{l}(r)$ is the center-of-mass radial distribution function in the $x$-$y$ plane, and $\tilde{g}_{nm}^{l}(r) \equiv [g_{nm}^{l}(r) + g_{mn}^{l}(r)]/2$. The radial distribution $g_{00}^{l}(r)$ shown in Fig. 3(b) exhibits some structure beyond the first peak indicating a certain degree of translational order. The circular harmonics $\tilde{g}_{20}^{l}(r)$ and $\tilde{g}_{22}^{l}(r)$ shown in Fig. 3(b) indicate orientational correlations extending to $\sim 18$ Å, and the negative values of $\tilde{g}_{20}^{l}$ correspond to a molecule perpendicular to the intermolecular axis, regardless of the orientation of its neighbor. The positive peak in $\tilde{g}_{22}^{l}$ corresponds to parallel intermolecular alignment and the first negative peak at $\sim 8$ Å to pairs of molecules in a T-like relative orientation.

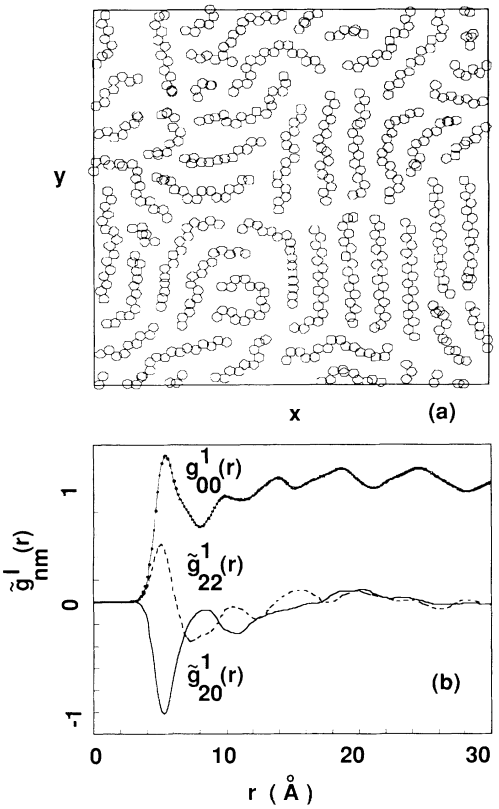


FIG. 3. (a) Typical structure in the plane of the first adsorbed layer of a $\sim 20$-Å-thick film (similar results obtained for all three film thicknesses). Note domains of intermolecular orientational (and translational) order. (b) Center-of-mass radial distribution function [$g_{00}^{l}(r)$, dotted solid line] and circular harmonics distributions [$\tilde{g}_{22}^{l}(r)$, dashed; $\tilde{g}_{20}^{l}(r)$, solid] in the first adsorbed layer of the 20-Å-thick film (similar results obtained for all three film thicknesses).

In the context of the molecular structure of the films it is of interest to comment on intramolecular dihedral conformations which exhibit dependence on distance from the solid surface. Thus for the first adsorbed layer of the $\sim 40$-Å-thick film the percentages of trans ($t$) and gauche dihedral configurations ($g_+$ and $g_-$) are 79, 10.7, and 10.3, respectively, while in the middle region of the film [of near bulk density, see Fig. 1(a)] and in the lv tail region $(t, g_+, g_-) = (66, 17, 17)$. Similar results, demonstrating enhanced trans conformations in the first adsorbed layer [3], were obtained for the other film thicknesses, correlating with the substrate-induced parallel-to-the-surface orientation of molecules in the layer, and the domains of intermolecular orientational alignment discussed above.

Finally, we note that the molecules in the film exhibit liquidlike, markedly anisotropic, diffusion constants with diffusion parallel to the surface greatly enhanced in the second layer of the thin two-layer film and in the tail region of the thick films [see Fig. 1(b)]. For the thinnest film the diffusion throughout the film is confined to two dimensions, and while $D_\perp = 0$ for molecules in the first adsorbed layer of the thicker films, it increases away from the sl interface (however, at the tail region $D_\parallel \sim 2.2 D_\perp$).

The results presented above constitute, to the best of our knowledge, the first microscopic theoretical characterization of adsorbed liquid films (beyond monolayer thickness [3]) of intermediate-length alkanes. In this size range the molecules possess a degree of complexity which differentiates them from simple, or short-chained, liquids, but they are too short to be considered as a polymer [10]. Consequently, a statistical mechanical treatment of such systems is complicated since neither the powerful general scaling ideas of polymer science [5] nor simple liquid theories are applicable to them. We hope that our results would stimulate further experimental and theoretical investigations of these systems, including the response of adsorbed films to interactions with probes such as those employed in tip-based microscopies [14,15], and rheological properties.

Useful conversations with W. D. Luedtke and R. N. Barnett are gratefully acknowledged. This research was

supported by the U.S. Department of Energy and the AFOSR. Calculations were performed at the Pittsburgh Supercomputer Center.

[1] O. Guiselin, L. T. Lee, B. Farnoux, and A. Lapp, J. Chem. Phys. **95**, 4632 (1991).

[2] See review by J. P. Rabe, in *Nanostructures Based on Molecular Materials*, edited by W. Gopel and Ch. Ziegler (VCH, Weinheim, 1992).

[3] S. Leggetter and D. J. Tildesley, Mol. Phys. **68**, 519 (1989).

[4] J. M. H. Scheutjens and G. J. Fleer, J. Phys. Chem. **84**, 178 (1980); J. S. Jones and P. Richmond, J. Chem. Soc. Faraday Trans. II **73**, 1062 (1977).

[5] P. G. de Gennes, *Scaling Concepts in Polymer Physics* (Cornell University, Ithaca, 1979); P. G. de Gennes, Macromolecules **14**, 1637 (1981); P. G. de Gennes and P. J. Pincus, J. Phys. (Paris), Lett. **44**, L241 (1983).

[6] E. Eisenreigler, K. Kremer, and K. Binder, J. Chem. Phys. **77**, 6296 (1982).

[7] (a) See review by A. Bonissent, in *Interfacial Aspects of Phase Transformations*, edited by B. Mutaftschiev (Reidel, Dodrecht, 1982); (b) U. Landman, C. S. Brown, and C. L. Cleveland, Phys. Rev. Lett. **45**, 2032 (1980); (c) J. Q. Broughton and G. H. Gilmer, J. Chem. Phys. **84**, 5759 (1986); (d) E. T. Chen, R. N. Barnett, and U. Landman, Phys. Rev. B **40**, 924 (1989); (e) J. D. Weeks, J. Chem. Phys. **67**, 3106 (1977).

[8] J. P. Ryckaert and A. Bellmans, Discuss. Faraday Soc. **66**, 95 (1978).

[9] The parameter $\sigma$ was obtained via the Lorentz-Berthelot mixing rule, $\sigma=(\sigma_{Au}+\sigma_{CH_2})/2$ with the pseudoatom $\sigma_{CH_2}=3.923$ Å and $\sigma_{Au}=2.637$ Å after T. Halicioglu and G. M. Pound, Phys. Status Solidi (a) **30**, 619 (1975). The LJ well depth $\epsilon=0.429$ kcal/mole was chosen to yield an adsorption energy of $\sim 1$ kcal/mole per pseudoatom unit, after results obtained via thermal desorption studies of alkanes adsorbed on metal surfaces [see Q. Dai and A. J. Gellman, Surf. Sci. (to be published); R. Zhang and A. J. Gellman, J. Phys. Chem. (to be published); A. V. Hamza and R. J. Madix, Surf. Sci. **179**, 25 (1987)].

[10] See H. K. Christenson, D. W. R. Gruen, R. G. Horn, and J. N. Israelachvili, J. Chem. Phys. **87**, 1834 (1987), in the context of surface force measurements of confined liquid *n*-hexadecane.

[11] J. N. Israelachvili, *Intermolecular and Surface Forces* (Academic, London, 1985), p. 158.

[12] J. J. Jasper, J. Phys. Chem. Ref. Data **1**, 841 (1972), see Table 51.2.

[13] M. W. Ribarsky and U. Landman, J. Chem. Phys. (to be published).

[14] C. M. Mate, M. R. Lorenz, and V. J. Novotny, J. Chem. Phys. **90**, 7550 (1989); C. M. Mate and V. J. Novotny, J. Chem. Phys. **94**, 8420 (1991).

[15] U. Landman, W. D. Luedtke, and E. M. Ringer, Wear **153**, 3 (1992).

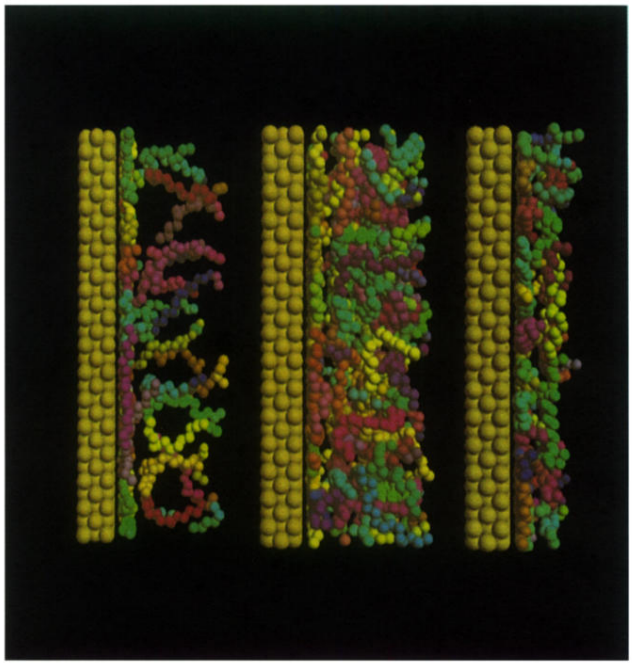

(a)

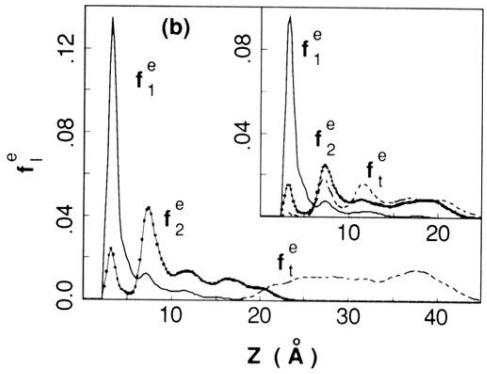


FIG. 2. (a) Molecular configurations of the thinnest (~10 Å, top) and intermediate thick (~20 Å, middle) adsorbed *n*-hexadecane films (side views). Molecules are differentiated by colors. Note the compactness of the first adsorbed layer at the sl interface, and the "rough" appearance of the lv interface. Shown at the bottom is a molecular configuration of the ~20-Å-thick adsorbed film depicting the first adsorbed layer, and only the bridging molecules with one end at the second layer and the other end located in the tail region (lv interface). (b) Conditional probabilities $f_l^e(z)$ for finding one end of a molecule in layer $l$, and the other end in a region about $z$, for the thick ($z \sim 40$ Å) adsorbed film. The dashed line corresponds to $f_t^e$, the probability for one end of the molecule to be located in the lv tail region and the other end about $z$ inside the film. Results for the intermediate thickness film (~20 Å) are shown in the inset.